

# **Necessity of *HuR/ELAVL1* for activation-induced cytidine deaminase-dependent decrease in topoisomerase 1 in antibody diversification**

Wajid Amin<sup>1</sup>, Shoki Nishio, Tasuku Honjo, and Maki Kobayashi<sup>1</sup>

Immunology and Genomic Medicine, Center for Cancer Immunotherapy and Immunobiology,  
Graduate School of Medicine, Kyoto University

606-8501, Kyoto City, JAPAN

<sup>1</sup> Both authors contributed equally

Correspondence to: T. Honjo; E-mail: honjo@mfour.med.kyoto-u.ac.jp

TEL +81 75 753 4371

FAX +81 75 753 4388

## Graphical Abstract

AID-dependent DNA cleavage are the initial event of antibody gene diversification. Using *HuR*-knockout (KO) CH12 cells, a B lymphoma cell line, it is revealed that deletion of *HuR* eliminates AID-dependent Top1 decrease. Since CSR impairment to IgG3 subclass in *HuR*-KO cells is rescued by knockdown of *Top1*, *HuR* is considered to be necessary for initiation of antibody diversification and acquired immunity by regulating AID-dependent reduction of Top1 protein and increasing DNA cleavage.

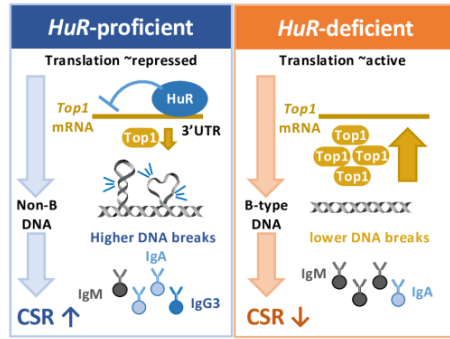
Accepted Manuscript

## Abstract

Activation-induced cytidine deaminase (AID)-dependent DNA cleavage are the initial event of antibody gene-diversification processes such as class switch recombination (CSR) and somatic hypermutation (SHM). We previously reported the requirement of an AID-dependent decrease of topoisomerase 1 (*Top1*) for efficient DNA cleavage, but the underlying molecular mechanism has remained elusive. This study focuses on *HuR/ELAVL1*, a protein that binds to AU-rich elements in RNA. *HuR*-knockout (KO) CH12 cells derived from murine B lymphoma cells were found to have lower CSR and hypermutation efficiencies due to decreased AID-dependent DNA cleavage levels. The *HuR*-KO CH12 cells do not show impairment in cell cycles and *Myc* expression, which have been reported in *HuR*-reduced spleen B cells. Furthermore, drugs that scavenge reactive oxygen species (ROS) do not rescue the lower CSR in *HuR*-KO CH12 cells, meaning that ROS or decreased c-Myc protein amount is not the reason for the deficiencies of CSR and hypermutation in *HuR*-KO CH12 cells. We show that *HuR* binds to *Top1* mRNA and that complete deletion of *HuR* abolishes AID-dependent repression of *Top1* protein synthesis in CH12 cells. Additionally, reduction of CSR to IgG3 in *HuR*-KO cells is rescued by knockdown of *Top1*, indicating that elimination of the AID-dependent *Top1* decrease is the cause of the inefficiency of DNA cleavage, CSR, and hypermutation in *HuR*-KO cells. These results show that *HuR* is required for initiation of antibody diversification and acquired immunity through the regulation of AID-dependent DNA cleavage by repressing *Top1* protein synthesis.

Keywords: AU-rich element, DNA cleavage, class switch recombination

## Graphical Abstract



## Introduction

Immunoglobulin (Ig) gene diversification in B lymphocytes is an essential immune mechanism for antibody memory formation, which enables efficient and rapid eradication of infectious organisms or neutralization of the produced toxins. Upon stimulation by non-self-antigens, activated B lymphocytes produce switched antibodies by class switch recombination (CSR), in which the constant ( $C_H$ ) region of Ig heavy (*IgH*) gene is exchanged from the  $C\mu$  to other downstream  $C_H$  regions, such as  $C\gamma$ ,  $C\epsilon$ , and  $C\alpha$ . This results in the conversion of surface IgM to IgG, IgE, and IgA, respectively (1,2). Furthermore, somatic hypermutation (SHM) occurs in the variable (V) region of the heavy and light chain genes to generate high-affinity antibodies against an encountered antigen.

Activation-induced cytidine deaminase (AID) is an essential enzyme for Ig gene diversification processes in vertebrates, including CSR, SHM, and gene conversion (GC) (3-5). Deficiency in AID causes a type of primary immunodeficiency, hyper-IgM syndrome type II (HIGM II), which involves a lack of switched antibodies other than IgM and high-affinity antibodies (5). CSR, SHM, and GC are initiated from AID-dependent cleavage at switch (S), V, and pseudo-V regions, respectively. There has long been debate about whether AID deaminates cytidine (C) in RNA or deoxycytidine (dC) in DNA (6). In the DNA deamination model, AID deaminates dC in the V or S region of the *IgH* gene and converts it into deoxy-uridine (dU) for DNA cleavage or SHM. However, we have proposed RNA editing by AID in that C in RNA is edited to uridine because the cytidine deamination domain of AID is conserved with that of other APOBEC RNA-editing enzymes. Furthermore, there have been several lines of evidence regarding UNG and APE1 that do not support the DNA deamination model (7-12), although the target of RNA editing of AID has not yet been identified (6).

We previously reported that AID reduces translation speed of topoisomerase 1 (Top1), decreases the amount of Top1 protein, and eventually facilitates the non-B DNA structure in the V and S regions of Ig loci, which are necessary for efficient CSR and SHM (13,14). From these results, we hypothesized that AID might edit some putative miRNA (or precursors) to reduce the translation of *Top1* mRNA. We searched for a protein that binds to *Top1* mRNA and regulates these steps. *Top1* mRNA includes many AU-rich elements (AREs) that mainly consist of AUUUA pentamers, so we focused on the RNA-binding proteins that bind to AREs.

ARE-mediated decay (AMD) of mRNA is one of the regulatory systems for mRNA stability that regulate the expression of factors such as growth factors, oncoproteins, and cytokines (15,16). AMD is reportedly linked with miRNA-mediated decay in several cases (16). AU-rich binding proteins contribute not only to the decay of some mRNAs, but also to the stabilization of other

mRNAs (17). For example, BRF1, KSRP, and TTP are known to destabilize some mRNAs that harbor AREs, while HuR (Human Antigen R)/ELAVL1 (Embryonic Lethal, Abnormal Vision, Drosophila-Like 1) reportedly stabilizes some mRNAs by binding to AREs. AUF-1/hnRNP D is involved in both regulatory directions of decay and stabilization of the target mRNAs. ARE-binding proteins are involved in the regulation of translation efficiency of binding mRNAs as well as degradation of mRNAs (17).

We investigated whether AMD is necessary for CSR and Top1 protein regulation by screening the major AU-binding proteins using knockdown methods in CH12 cells derived from mouse B lymphoma. We found that knockdown of HuR decreased CSR to IgA. Based on this result, we utilized CH12 cells to completely knockout (KO) the *HuR* gene and investigated the regulation of Top1 by HuR. We identified the disturbed regulation of Top1 protein synthesis in *HuR*-KO cells and rescue of CSR to IgG3 by enforced reduction of Top1 using knockdown. Our findings show that HuR specifically regulates AID-dependent DNA cleavage mechanisms and immunological memory by binding to *Top1* mRNA and regulating Top1 protein synthesis.

## Methods

### *Cell culture*

CH12F3–2A cells were cultured and stimulated for induction of CSR and hypermutation in 5' region of S $\mu$  region (5'S $\mu$ ) as described previously (13,18). Briefly, endogenous AID was induced by the combination of CD40L (laboratory-made), IL-4 (Fujifilm, Tokyo, Japan) (CI), or CI plus TGF- $\beta$  (R&D systems, Minneapolis, USA) (CIT). Exogenous AID-ER (AID fused with estrogen receptor ligand binding domain) was activated by 4-hydroxytamoxifen (4-OHT, Sigma-Aldrich, St. Louis, USA).

### *Primary mouse splenic B cells and mouse neuronal tissues*

Spleen cells isolated from 10-week-old wild-type and AID knockout C57BL/6 mice were cultured as described previously (4) with LPS or a combination of LPS with IL4, TGF- $\beta$  or murine IFN- $\gamma$  (Peprotech in Thermo Fisher Scientific, Waltham, USA) for 96 hours. The cultures with LPS with IL4 were used for detection of IgG1 and IgE, those with LPS with IFN- $\gamma$  were for IgG2a, and those with LPS with TGF $\beta$  were for IgG2b and IgA. IgG3 was detected in the culture stimulated only by LPS. These *in vitro* cultured splenic B cells were used for assays of surface immunoglobulin (Ig), post-

switch transcripts, and RNA-IP. Cerebral cortex and spinal cord tissues were recovered from a wild-type C57BL/6 mouse.

### *Knockdown of ARE binding factors and Top1 with CRISPR-interference (CRISPRi) or siRNA in CH12 cells*

Lentivirus supernatant was generated with the lentiviral construct pLKO5d.SFFV.dCas9-KRAB.P2A.BSD, which was a gift from Dirk Heckl (Addgene plasmid # 90332; <http://n2t.net/addgene:90332>; RRID:Addgene\_90332) (19). Transfected CH12 cells were selected by blasticidin (BSD) and limitedly diluted to raise monoclonal cells that stably express dCas9-KRAB (CH12-dCas9-KRAB#40). The online guideRNA (gRNA) design tools CHOPCHOP (20), CRISPOR (21), and CRISPick (22,23) were used to select gRNA sequences against *Brf1*, *Brf2*, *hnRNPD*, *Khsrp*, and *Zfp36*. The gRNA sequences are described in **Supplementary Table 1**.

Double strand oligos (Eurofins Genomics, Luxembourg) were annealed and cloned into pSPgRNA, which was a gift from Charles Gersbach (Addgene plasmid # 47108; <http://n2t.net/addgene:47108>; RRID:Addgene\_47108) (24). The constructed plasmids' sequences were verified by Sanger sequencing (BigDye Terminator v3.1 and 3130xl Genetic Analyzer, Thermo Fisher Scientific). gRNA plasmids were transiently transfected in CH12-dCas9-KRAB#40 cells. The cells were stimulated by CIT stimulation at 48 hours after transfection and evaluated for IgA expression after 24 hours incubation.

Knockdown efficiency was analyzed by reverse transcription-polymerase chain reaction (RT-PCR). RNA was purified by Sepasol RNA Super II (Nacalaitesque, Kyoto, Japan) or a Maxwell RSC simplyRNA Cells Kit (Promega, Madison, USA). cDNA was synthesized with SuperScript IV Reverse Transcriptase (Thermo Fisher Scientific), and the sequences of the RT-PCR primers are described in **Supplementary Table 1**.

To knockdown *HuR*, two Stealth RNAs were custom-designed (Thermo Fisher Scientific), and their sequences are shown in **Supplementary Table 1**. The Stealth RNA oligos and *Top1* knockdown method to CH12 cells were applied as reported previously (13).

### *HuR knockout cell generation*

*HuR*-KO cell lines were generated from wild-type CH12 cells by the CRISPR/Cas9 technique, as described previously (25). Briefly, three different gRNA-producing plasmids were generated based on the vector pX335-U6-Chimeric\_BB-CBh-hSpCas9n(D10A), which was a gift from Feng Zhang (Addgene plasmid # 42335; <http://n2t.net/addgene:42335>;

RRID:Addgene\_42335) (26). Serial transfection of two targeting vectors containing zeocin (Zeo) and blasticidin (BSD)-resistant gene cassettes replaced Exons 3 and 4 of the *ELAVL1* gene to abolish the full-length HuR protein expression (**Supplementary Figure 1A**). This was done by electroporation using an Amaxa SF Cell Line 96-well Nucleofector Kit (96 RCT) (Lonza, Basel, Switzerland) and following the manufacturer's instructions.

**Supplementary Table 1** shows the primers and DNA polymerases used for generating gRNA plasmids, targeting vectors, and genotyping. Drugs used for the cell selection are listed in **Supplementary Table 1**. Multiple cell lines with transfected molecules were used in this study and are summarized in **Supplementary Table 2**.

#### *Overexpression of HuR and AID-ER*

Electroporation method was used to transfect *HuR* or *AID-ER* constructs in CH12-derived *HuR* KO cells as described previously (13). *AID-ER* IRES ZsGreen-transfected cells were sorted by a FACS Aria II (BD Biosciences, Franklin Lakes, USA) based on their high fluorescence intensity and limitedly diluted to isolate the monoclonal cells.

#### *Flowcytometry analysis*

Western blot and flowcytometry analyses were done using the antibodies listed in **Supplementary Table 1**. The mouse spleen B cells were blocked with the purified anti-mouse CD16/32 (BioLegend, San Diego, USA). The CH12 cells and the spleen B cells were stained by biotinylated anti- IgG1 (BioLegend), IgG2a (BD, Franklin Lakes, USA), IgG2b (BD), IgG3 (BD) and IgE (BD) antibodies. These cells were washed and stained by PE-conjugated streptavidin (BioLegend). PE-conjugated IgA antibody (Southern Biotech) was used to detect surface IgA in the CH12 and the spleen B cells. Cellular fluorescence was evaluated by a FACS Calibur (BD).

#### *Analyses of CSR and hypermutation in 5'S $\mu$*

CSR and hypermutation in 5'S $\mu$  were performed as described previously (11,13). In the hypermutation analysis, the reference sequence basically was taken from the GRCm38 database (mm10), but CH12-specific allelic mutations that are shared among many sequencing reads were omitted from AID-dependent mutation counts.



### *RT-PCR*

RNA was purified by Sepasol Super II (Nacalaitesque) or Maxwell RSC (Promega) with a Maxwell RSC simplyRNA Cells Kit (Promega). RT-PCR was performed as described previously to detect  $\mu$ - and  $\alpha$ -germline transcripts (*GLT*), the other mRNAs, and post-switch transcripts (13). Quantitative PCR was performed using PowerUp SYBR Green Master Mix (Thermo Fisher Scientific) and an Applied Biosystems 7900HT Fast Real-Time PCR system (Applied Biosystems, Waltham, USA). Alternative splicing of dihydrolipoamide S-succinyl transferase (*Dlst*) mRNA was also detected by conventional RT-PCR. The primers used are described in **Supplementary Table 1**.

### *Western blot*

Protein samples were basically prepared as described previously (13) in RIPA buffer (20 mM Tris-Cl, pH 8.0, 150 mM NaCl, 1% TritonX-100, 0.5% deoxycholate, 0.1% sodium dodecyl sulphate) with 2 M urea, followed by sonication using a Bioruptor (BMBio, Tokyo, Japan). Western blot analysis was also performed as described previously. Soluble Top1 protein was isolated by PBS-TritonX100 (PBS with 0.1% TritonX-100) with sonication, centrifuged, and mixed with 25% 5X Laemli buffer (312.5 mM Tris-HCl pH 6.8, 10% SDS, 50% glycerol, 0.02% bromophenol blue, and 250 mM DTT). The antibodies used in western blot analysis are shown in **Supplementary Table 1**.

### *DNA break assay labeling with biotinylated d-UTP (bio-dUTP) by terminal deoxy-transferase (TdT)*

This assay is performed following the published method with minor modifications (27). Briefly, the fixed  $5 \times 10^6$  cells were washed with the buffer D [100 mM Tris-HCl (pH7.4), 150 mM NaCl] and T4 polynucleotide kinase (PNK) buffer (New England Biolabs, Massachusetts, USA), the cells were incubated with T4 PNK (New England Biolabs #M0201L) in PNK buffer for 1 hour at 37°C. After washing with buffer D and terminal deoxynucleotidyl transferase (TdT) buffer (TaKaRa, Kyoto, Japan) with BSA (TaKaRa), the cells were treated by TdT with bioin-16-dUTP (MERCK, Darmstadt, Germany) for 1 hour at 37°C. After washing with buffer D, treatments with 2  $\mu$ l of RNase A (Nippongene, Tokyo, Japan) in 100  $\mu$ l of buffer D at 37 °C for 20 min and 0.2 mg/ml ProK (MERCK) in 500  $\mu$ l of the lysis buffer [10 mM Tris-HCl (pH8.0), 10 mM EDTA, 150 mM NaCl, 0.1% SDS] at 55°C for overnight followed. The DNA is fragmented by sonication with Bioruptor (Sonicbio, Kanagawa, Japan) into 500 - 2,000 bp length and purified by addition of 250  $\mu$ l of 5M NaCl, centrifuge for 5 min at 15,000 rpm, and precipitation with the equal amount of 2-propanol. 20  $\mu$ g of

DNA was trapped by 10  $\mu$ l of Dynabeads MyOne Streptavidin C1 (Thermo Fisher Scientific) blocked with BSA (MERCK) in the trapping buffer [5 mM Tris-HCl (pH 7.4), 0.5 mM EDTA, 0.02% Tween20]. After overnight incubation at 4°C, the beads were washed with low-salt RIPA [50 mM Tris-HCl (pH 8.0), 150 mM NaCl, 10 mM EDTA, 1% TritonX-100, 0.1% SDS, 0.1% DOC], high-salt RIPA [50 mM Tris-HCl (pH 8.0), 1 M NaCl, 10 mM EDTA, 1% TritonX-100, 0.1% SDS, 0.1% DOC] and LiCl wash [20 mM Tris-HCl (pH 8.0), 0.25 M LiCl, 1 mM EDTA, 0.5% NP-40, 0.5% DOC] buffers for three times. The trapped DNA was eluted by 98  $\mu$ l formamide and 2  $\mu$ l of 0.5M EDTA and precipitated by 2-propanol and 0.2M NaCl with glycogen. The trapping efficiency was evaluated by qPCR. The primers used are listed in **Supplementary Table 1**.

#### *Cell proliferation assay*

The cell proliferation assay was performed with a CellTrace Violet (CTV) Cell Proliferation Kit (Thermo Fisher Scientific) using the manufacturer's instructions with minor modification. Briefly,  $5 \times 10^6$  cells were labeled with 0.6  $\mu$ M CTV, cultured with or without CIT, and the CTV intensity was measured by a FACS Canto II (BD Biosciences) at 24 hours after labeling. Aphidicolin was used to stop replication (Sigma-Aldrich). N-acetyl-L-cysteine (L-NAC) (Sigma-Aldrich) and EUK-134 (Sigma-Aldrich) were used to test the effect of ROS on the CSR efficiency and cell death. After 2 hours of incubation of the cells with 0-50 mM L-NAC or 0-10  $\mu$ M EUK-134, CIT stimulation was started, and the cell-surface IgA expression was evaluated after 24 hours.

#### *RNA-IP of HuR*

RNA-IP was performed by following previous publications (28,29) with minor modifications. Dynabeads Protein G (Thermo Fisher Scientific) were washed with NT2 buffer (50 mM Tris-HCl (pH7,4), 150 mM NaCl, 1 mM MgCl<sub>2</sub>, 0.05% NP-40, and 5 mM EDTA) and precoated with anti-ELAVL1 antibody or normal IgG with blocking reagents (500  $\mu$ g/ml BSA (NEB), 200  $\mu$ g/ml HS-DNA (Thermo Fisher Scientific), and 200  $\mu$ g/ml glycogen (NEB)) overnight at 4°C. The washed beads were incubated with the cell lysate supplemented with RNaseOUT for 3 hours at 4°C. The beads were washed with NT2 buffer four times and divided into two parts for protein and RNA extraction (10% and 90%, respectively). RNA was extracted using Sepasol RNA II Super (Nacalaitesque), and cDNA was synthesized with SuperScript IV Reverse Transcriptase (Thermo Fisher Scientific). qPCR was conducted as described in the *RT-PCR* section.

### *Polysome fractionation*

Polysome analysis was performed as previously reported with minor modifications (30). Briefly, a 10-45% sucrose gradient with 0.1 µg/ml cycloheximide (CHX) was produced using GradientMaster (BioComp Instruments, Fredericton, Canada).  $4 \times 10^7$  cells were lysed in polysome lysis buffer supplemented with 1 mg/ml CHX and loaded in the sucrose gradient. Ultracentrifuging with a P40ST rotor (Hitachi, Hitachi, Japan) was performed at 25,400 rpm (81 kg) for 2 hours at 4°C. This condition was less than the typical condition (222 kg) for polysome fractionation because we aimed for the clear separation of *Top1* mRNA.

Polysome fractions were recovered by a Piston Gradient Fractionator (BioComp Instruments) at a speed of 0.3 cm/sec and distance of 0.9 mm for each fraction. The fraction number per sample obtained was 90. The optical density at 256 nm (OD 256 nm) was measured for each fraction. RNA was extracted from the pools of the 10 serial fractions and analyzed as described previously using *RT-PCR* section. The qPCR signal of each pool of fractions was normalized by the input signal of each sample.

### *Re-analysis of the published data*

iCLIP data obtained using anti-HuR antibody (GSE62148) by Diaz-Muñoz *et al.* were downloaded (31) and mapped to the UCSC Genome Browser to see the enrichment of *Top1* mRNA by HuR in the mm10 mouse genome.

## **Results**

### *Screening of ARE-binding proteins contributing to CSR identified HuR*

*Top1* mRNA includes multiple ARE motifs, among which **Supplementary Table 3A** summarizes the ATTTA or WTTTW (W=A or T) included in 3' untranslated region (*UTR*) of mouse *Top1* mRNA. Some of these motifs are conserved throughout vertebrates. We hypothesized that an ARE-binding factor may support the AID-dependent *Top1* decrease.

To identify the ARE-binding factors that are necessary for CSR to IgA, we evaluated the CSR efficiency after knockdown of *Brf1*, *Brf2*, *hnRNPD*, *Khsrp*, *Zfp36*, and *HuR* by CRISPRi (32) or

RNAi. Out of four ELAV family proteins, HuB, HuC, HuD and HuR, only HuR was expressed in murine B lymphoma-derived CH12 cells as previously reported (**Supplementary Figure 2**) (33,34). Therefore we selected HuR as a candidate Hu protein for binding to Top1 mRNA. Of these ARE-binding factors, about 30% expression of *HuR* compared to the control resulted in ~50% of CSR to IgA, while  $2.8 \pm 0.7\%$  of *Brf2* expression resulted in ~60% (**Fig. 1A-B**). The expression level of the *aicda* gene and the  $\mu$ - and  $\alpha$ -germline transcripts (*GLT*) was not affected by knockdown of *HuR*, whereas *Brf2* knockdown modestly downregulated *aicda* expression (**Fig. 1C-D**).

#### *Gene targeting and rescue of HuR in CH12 cells verified the necessity of HuR for CSR*

Based on the screening results of ARE-binding factors (**Fig. 1**), *HuR* was selected for further investigation. To elucidate the molecular function of HuR in AID-dependent *IgH* gene diversification, *HuR*-KO CH12 cells were generated by CRISPR/Cas9 technique (**Supplementary Figure 1A**). Genotyping PCR of several clones revealed the expected band size derived from the recombined alleles with Zeo or BSD (**Supplementary Figure 1B-C**). CSR of these *HuR*-KO cells is generally low at approximately less than half that in wild-type (WT) CH12 cells (**Supplementary Figure 1D**). Three clones showed higher efficiency of CSR among the obtained several *HuR*-KO cell lines: #101, #110, and #111. These were used for further analyses to avoid picking up cells with less AID or less  $\mu$ - and  $\alpha$ -GLTs.

Loss of *HuR* seems to cause lower CSR efficiency since the CSR to IgA (IgA-CSR) in all the *HuR*-KO cell lines is less than half that of the WT CH12 cells (**Supplementary Figure 1D**). We sought to confirm whether the amount of HuR positively correlates with the level of CSR and to exclude the possibility of off-target effect by gene targeting. Thus, bi-cistronic vector expressing *HuR* cDNA and a puromycin-resistant gene or an empty vector was stably transfected in *HuR*-KO clones, as shown in **Fig. 2A**. IgA expression was recovered by overexpression of exogenous HuR in both #101 and #111 cell lines at 24 and 48 hours (**Fig. 2B**). *HuR*-deficient (*HuR*<sup>-</sup>) cells showed CSR with 4-5 times less efficacy than *HuR*-proficient (*HuR*<sup>+</sup>) cells in both the #101 and #111 cell lines at 24 hours after stimulation by a cytokine cocktail (CIT). At 48 hours, the CSR efficiency in *HuR*<sup>-</sup> cells were 2-3 times less than that in *HuR*<sup>+</sup> cells as well. This result indicates that the amount of HuR protein contributes to the CSR efficiency.

*HuR is necessary for CSR and Hypermutation in 5'S $\mu$  region by regulation of AID-dependent DNA cleavage*

We introduced an AID-ER IRES ZsGreen vector to the cell lines to obtain the *HuR*<sup>-</sup> and *HuR*<sup>+</sup> cells that harbor equally functional AID. As a result, we isolated clones #22B (*HuR*<sup>-</sup>) and #11A (*HuR*<sup>+</sup>), which express almost equal levels of exogenous AID-ER and endogenous AID upon stimulation by CIT and 4-OHT, respectively (**Supplementary Figure 3A-C**). These *HuR*<sup>-</sup> and *HuR*<sup>+</sup> cell lines show different CSR efficiency in both endogenous (AID) and exogenous (AID-ER) modes of AID activation, as the #101 and #111 cell lines showed (**Supplementary Figure 3D-E**). They also show similar levels of  $\mu$ - and  $\alpha$ -GLTs (**Supplementary Figure 3F**).

Whereas cell-surface IgA is generally detected to monitor the CSR efficiency in CH12 cells, cell-surface IgG3 is also reportedly expressed by AID activation in CH12 cells (35). To see the difference in CSR capability between *HuR*<sup>-</sup> and *HuR*<sup>+</sup> cells in a class other than IgA, CSR to IgG3 (IgG3-CSR) was also detected in stimulated *HuR*<sup>-</sup> and *HuR*<sup>+</sup> cells. TGF $\beta$  stimulates  $\alpha$ -GLT transcription and promotes the switch to IgA (36), so a combination of CD40L and IL-4 (CI stimulation) without TGF $\beta$  was used to induce CSR in addition to CIT stimulation.

As expected, the rates of IgA-CSR in *HuR*<sup>-</sup> cells were only  $\times 1/11 \sim 1/7$  and  $\times 1/4 \sim 1/2$  of that in *HuR*<sup>+</sup> cells in CI and CIT stimulation ( $P < 0.001$ ) during days 1-3, respectively (**Fig. 2C-D**). The IgA-switched cell percentage was higher in the CIT-stimulated cells than the CI-stimulated cells, but IgG3 switching was induced much more in the CI-stimulated cells than in the CIT-stimulated ones in days 2-3 (**Fig. 2E**). The difference in IgG3 expression between *HuR*<sup>-</sup> and *HuR*<sup>+</sup> cells is also obvious because CI-induced IgG3 expression in *HuR*<sup>-</sup> cells reached only  $\times 1/9 \sim 1/8$  of that in *HuR*<sup>+</sup> cells ( $P < 0.001$ ). To find the difference of CSR capability between *HuR*<sup>-</sup> and *HuR*<sup>+</sup> cells furthermore, we evaluated the expression of the other classes of surface Ig (sIg), IgG1, IgG2a, IgG2b and IgE in WT and AID knockout (AIDKO or A-KO) CH12 cells (**Supplementary Figure 3H-I**). While mouse WT spleen B cells showed sIg expression of the other classes by the several modes of stimulation, WT CH12 cells show no substantial sIg expression other than IgA and IgG3 within 40 hours (**Supplementary Figure 3H-I**). To evaluate this expression pattern more accurately, we also checked the post-switch transcripts, starting from I $\mu$  promoter and spliced to the downstream constant regions after class switch recombination (4). In consistent with the sIg expression pattern, WT CH12 cells did not show any practical post-switch transcripts except for I $\mu$ F-I $\alpha$ R and I $\mu$ F-I $\gamma$ 3R (**Supplementary Figure 3J**), while these post-switch transcripts were observed in WT mouse spleen B cells cultured *in vitro* (**Supplementary Figure 3K**). By these reasons, we only evaluated IgA or IgG3 expression in the following experiments.

CSR depends on multiple factors that regulate cleavage and repair steps of DNA, so the exact target step of *HuR* deficiency was still unclear. Therefore, *HuR*<sup>-</sup> and *HuR*<sup>+</sup> cells were compared using the hypermutation frequency in 5' of the *Sμ* core region, the other mode of AID-dependent *IgH* gene diversification (**Fig. 2F-G**). The cells were stimulated by both CIT and 4-OHT for induction of endogenous AID and exogenous AID-ER, respectively, and the DNA samples were recovered at 48 hours after the start of stimulation. The 36-51 kilobase pairs from 67-94 clones for each sample were used for hypermutation analyses, as shown in **Table 1**.

The hypermutation frequency in CIT-stimulated *HuR*<sup>-</sup> cells was  $3.9/10^4$  bp, which is significantly lower than the value of  $8.9/10^4$  bp in CIT-stimulated *HuR*<sup>+</sup> cells. The hypermutation frequency in 4-OHT-stimulated *HuR*<sup>-</sup> cells was also significantly lower ( $2.6/10^4$  bp) compared to that in *HuR*<sup>+</sup> cells ( $7.9/10^4$  bp) ( $P < 0.01$  and  $P < 0.001$  in CIT-stimulated and 4-OHT-stimulated cells by Fisher's exact test, respectively; **Fig. 2G and Table 1**). The base replacement profiles in this hypermutation assay were not different between *HuR*<sup>-</sup> and *HuR*<sup>+</sup> cells (**Supplementary Table 4**).

The hypermutation process requires AID-dependent, single- or double-strand DNA breaks (SSBs and DSBs), because hypermutation is the footprint of the error-prone DNA polymerases such as polymerase zeta or polymerase iota that repairs SSBs and DSBs (6,37). This idea is supported by evidence that SHM largely depends on the error-prone polymerases (38-40). Therefore the DNA cleavage step that is shared between CSR and hypermutation was hypothesized to be the target of *HuR*-deficiency. We detected DNA break efficiency by DNA break assay labeling with biotinylated d-UTP (Bio-dUTP) by terminal deoxy-transferase (TdT) (**Fig. 2H**) in *HuR*<sup>-</sup> and *HuR*<sup>+</sup> cells. This assay utilizes TdT, which adds nucleotide to 3' SSB ends without template and allows detection of SSBs. As a result, SSB frequency in *HuR*<sup>-</sup> cells showed two times to three times less signals than that in *HuR*<sup>+</sup> cells, indicating that the DNA cleavage step is the target of *HuR* deletion. The negative controls, *AIDKO* cells labeled with Bio-dUTP and CIT-stimulated *HuR*<sup>+</sup> cells without labeling did not show meaningful signals.

#### *Cell proliferation defects or ROS stress does not cause lower CSR efficiency in HuR-KO CH12 cells*

Impairment of cell proliferation was observed in previously reported *HuR*-conditional knockout (cKO) spleen B cells, in which *HuR* was deleted by Mb1-Cre or AID-Cre (31,41). We tested whether this finding is reproduced *in vivo* in the cultured CH12 cells by measuring proliferation rate of *HuR*<sup>-</sup> and *HuR*<sup>+</sup> cells with or without CIT stimulation using CellTrace Violet (CTV) dye and flowcytometric detection (**Fig. 3A-C**). IgA-CSR in *HuR*<sup>-</sup> and *HuR*<sup>+</sup> cells labeled with CTV (**Figure 3B**) showed the consistent level of IgA-CSR compared to the non-labeled cells as shown in **Figure 2D**. The flow cytometric pattern of CTV stained shows no delay in cell division in *HuR*<sup>-</sup> cells

compared to that in *HuR*<sup>+</sup> cells throughout the three experiments (**Fig. 3C, Supplementary Figure 4A**). Aphidicolin-treated cells showed the proliferation delay as expected.

Additionally, the cell cycle-related factors of mRNA expression were tested in both *HuR*<sup>-</sup> and *HuR*<sup>+</sup> cells (**Supplementary Figure 4B**). Except for the *cyclinD1* and *citrate synthase (CS)* genes which harbors multiple AREs in their 3'UTR (42) (**Supplementary Figure 4C**), *HuR*<sup>-</sup> cells showed no decrease in expression of these mRNAs.

To evaluate the influence of reactive oxygen species (ROS) accumulation in *HuR*<sup>-</sup> cells more directly, the response to the ROS scavenger drugs N-acetyl-L-cysteine (L-NAC) and EUK-134 was examined in *HuR*<sup>-</sup> and *HuR*<sup>+</sup> cells derived from *HuR*<sup>-</sup> cell line #111 (**Fig. 3D-F, Supplementary Figure 4D-F**). The dead cell fraction was estimated using the forward scattered (FSC) and side scattered (SSC) distribution pattern (**Supplementary Figure 4D**). Neither L-NAC nor EUK-134 rescued the lower IgA% in *HuR*<sup>-</sup> cells (**Fig. 3E-F, Supplementary Figure 4E**). Instead, L-NAC decreased IgA% and increased the dead cell population with the increase in drug concentration (**Fig. 3E**). These effects are probably caused by the acidic pH change of the culture medium from the higher concentration of L-NAC (**Supplementary Figure 4F**). These results suggest that the decrease of CSR to IgA and IgG3 in *HuR*<sup>-</sup> cells is not caused by the accumulation of ROS in CH12.

Although ROS stress does not affect CH12 cells' phenotypic fitness, the regulation of ROS stress genes is examined in CH12 cells as well as primary B cells (31) at the molecular level. Splicing of dihydrolipoamide S-succinyl transferase (*Dlst*) mRNA was reportedly disturbed in the spleen B cells derived from *HuR*-conditional knockout mouse, downregulating ROS stress response. In *HuR*-CH12 cells, *Dlst* mRNA showed increased intron inclusion (**Fig. 3G**), while aberrant Exon 10b (31) was not detected by conventional RT-PCR (**Fig. 3H**). Accordingly, *Dlst* protein expression was decreased in *HuR*<sup>-</sup> cells, as reported (**Fig. 3I**), showing that *Dlst* expression is positively regulated by *HuR* in CH12 cells. On the other hand, c-Myc protein expression was not changed by the absence of *HuR* (**Fig. 3J**), which was previously reported in primary B cells with decreased HuR (41). Overall, CH12 cell-cycle regulation and c-Myc protein level are not affected by *HuR* deletion, whereas *HuR*<sup>-</sup> cells showed disturbed splicing of the *Dlst* mRNAs and altered expression of *Dlst* protein.

#### *HuR is necessary for AID-dependent repression of Top1 protein synthesis*

We previously showed that a decrease in the amount of Top1 protein is necessary to cause AID-dependent CSR and hypermutation (13,14). HuR is reported to cooperate with miRNA machinery to suppress the translation of target mRNA by binding (43). Furthermore, re-analysis of the published data by Diaz-Muñoz et al. (31) shows the binding of HuR to 3' UTR of *Top1* mRNA (**Supplementary**

**Figure 5A**). Therefore, HuR was hypothesized to repress the level of Top1 protein by binding to *Top1* mRNA.

To test this possibility, the soluble Top1 protein level was examined in CI- and CIT-stimulated *HuR*<sup>-</sup> and *HuR*<sup>+</sup> cells (**Fig. 4A, Supplementary Figure 5B**). Three independently repeated experiments with samples recovered in PBS-TritonX-100 buffer showed that the decrease in Top1 protein by AID-activation did not occur in *HuR*<sup>-</sup> cells, while did occur in *HuR*<sup>+</sup> cells. On the other hand, the total amount of Top1 protein in the whole cells extracted by RIPA buffer did not show any difference between stimulated and not stimulated *HuR*<sup>-</sup> and *HuR*<sup>+</sup> cells (**Fig. 4B**), meaning that the AID-dependent decrease of Top1 is specific to the soluble fraction. Furthermore, the amount of *Top1* mRNA was not different between *HuR*<sup>-</sup> and *HuR*<sup>+</sup> cells (**Fig. 4C**), suggesting that the AID-dependent decrease of Top1 protein is post-transcriptionally regulated.

To confirm whether HuR binds to *Top1* mRNA in CH12 cells, RNA-IP with anti-HuR antibody was performed using #11A *HuR*<sup>+</sup> cells (**Fig. 4D-F and Supplementary Figure 5C-E**) and WT mouse splenic B cells (**Fig. 4G-H and Supplementary Figure 5F-H**). The positions of the primers (from *a* to *h*), designed to include the particular eight ATTTA motifs (circled number 1 to 8) in their amplicons, are shown in **Fig.4D and Supplementary Table 3B**. IP efficiency is sufficiently specific in every experiment, as shown in the western blot pictures (**Fig. 4E and 4G, Supplementary Figure 5D and 5G**). In CH12 cells, *Top1* 3' UTR-*h* primer sets revealed that *HuR* binding to *Top1* mRNA occurs more in CIT-stimulated cells than in non-stimulated cells, whereas *HuR* binding to *c-Myc* mRNA is not changed upon stimulation (**Fig. 4F, Supplementary Figure 5E**). To see whether this *HuR*-binding to *Top1* mRNA is reproduced in the mouse primary B cells, RNA-IP assay using anti-HuR antibody was repeated in WT and AIDKO cells stimulated by LPS and IL4 for four days. While ~ 30% of the WT spleen B cells switched into IgG1, AIDKO spleen cells did not switch (**Supplementary Figure 5F**). As a result, *HuR* is recruited to *Top1* mRNA, especially in the distal end of 3'UTR, shown by the primer set 3'UTR-*h* (**Fig.4H, Supplementary Figure 5H**). As it was shown in CH12 cells, AID-activated WT spleen B cells also show more strong recruitment of *HuR* to *Top1* 3'UTR compared to AIDKO B cells.

The translational level of *Top1* was evaluated by three independent polysome fractionation experiments (**Fig. 4I-M, Supplementary Figure 6**). OD 256 nm profiles showed that *HuR*<sup>-</sup> and *HuR*<sup>+</sup> have no gross difference in global translation efficiency (**Fig. 4I-J and Supplementary Figure 6B**). CIT also does not affect general translation efficacy. While the *Top1* mRNA in a heavy, highly translated fraction is remarkably decreased by CIT stimulation in *HuR*<sup>+</sup> cells (**Fig. 4L and Supplementary Figure 6C**), the *Top1* mRNA distribution in the heavy fractions is not decreased by CIT stimulation in *HuR*<sup>-</sup> cells (**Fig. 4K and Supplementary Figure 6C**). *β2M* mRNA distribution is not altered upon CIT stimulation and is also not different between *HuR*<sup>-</sup> and *HuR*<sup>+</sup> cells (**Fig. 4M-N**



and Supplementary Figure 6C). These results are consistent with the necessity of HuR in the AID-dependent decrease of Top1 protein (Fig. 4A).

### Knockdown of Top1 rescues the impaired CSR in HuR-KO cells

We speculated that low CSR efficiency in *HuR*<sup>-</sup> cells is caused by the elimination of AID-dependent Top1 decrease. Therefore, we tested whether forced reduction of Top1 amount using Top1 knockdown (*siTop1*) in *HuR*<sup>-</sup> cells equalizes the CSR efficiency in *HuR*<sup>-</sup> cells and that in *HuR*<sup>+</sup> cells.

The electroporation procedure of *siTop1* was repeated for three times every three days and followed by CI or CIT stimulation 24 hours after the last electroporation (Fig.5A). IgA% and IgG3% were detected on Day1-3 from the start of the stimulations.

Top1 protein amounts were sufficiently decreased by *siTop1* in both *HuR*<sup>-</sup> and *HuR*<sup>+</sup> cells (Fig.5B). AID-dependent decrease in Top1 protein was not detected by western blot after the repeated *siTop1* procedure. Because repeated *siTop1* procedure modestly increased the level of IgA% and IgG3% even in non-stimulated cells (no stim., in both *HuR*<sup>-</sup> and *HuR*<sup>+</sup> cells, Fig.5C), AID-dependent CSR level in CI- or CIT-stimulated cells was calculated by subtracting IgA% or IgG3% in unstimulated cells (AID-dependent IgA% and AID-dependent IgG3%, in Fig.5D-E).

Under CIT-stimulation, IgA-CSR in *siTop1-HuR*<sup>-</sup> cells was increased to the close level to that in *siTop1-HuR*<sup>+</sup> cells on Day3 (P value = 0.078, Fig.5D). This rescue of CSR deficiency in *HuR*<sup>-</sup> cells by *siTop1* is more pronounced in IgG3-CSR detection than IgA-CSR detection (Fig.5E). Without *siTop1*, IgG3% in stimulated *HuR*<sup>-</sup> cells is almost none after subtraction of IgG3% in non-stimulated cells. It is noteworthy that addition of *siTop1* to *HuR*<sup>-</sup> cells upregulates IgG3-CSR from the background level into the similar level to *siTop1-HuR*<sup>+</sup> cells in both CI- and CIT-stimulation modes. However, the IgA-CSR by CI-stimulation in *siTop1-HuR*<sup>-</sup> cells remains significantly lower than *siTop1-HuR*<sup>+</sup> cells. This reveals that rescue effect on IgA-CSR by *siTop1* is partial, probably because HuR is necessary for IgA-CSR by regulating the other mechanism than Top1 protein synthesis.

## Discussion

By screening major ARE-binding factors that potentially bind to ARE motifs in *Top1* mRNA, we discovered the requirement for HuR in efficient AID-dependent DNA cleavage. The results confirmed that HuR is necessary for CSR in CH12 cells. Furthermore, we showed that HuR binds to *Top1* mRNA and supports AID-dependent suppression of Top1 protein synthesis. Knockdown of *Top1* could recover the inefficiency of IgG3-CSR and compensate for the effect of *HuR* deletion, while this rescue remains partial in IgA-CSR. The repeated *siTop1* procedure decreases the amount of Top1 protein to the minimum level and may alter the "insufficient non-B DNA" in *HuR*<sup>-</sup> cells to "sufficient non-B DNA" (**Fig. 6**). This structural alteration of DNA possibly upregulates and rescues IgG3-CSR in *siTop1*-treated *HuR*<sup>-</sup> cells to a level equal to that in *siTop1*-treated *HuR*<sup>+</sup> cells. These results suggest that Top1 protein is at least partly important as a regulatory target of *HuR* in the process of AID-dependent DNA cleavage and CSR.

HuR is a 326-a.a. protein and one of the ELAV family of proteins that harbor three RNA recognition motifs (RRMs) and a nuclear-cytoplasmic shuttling domain (34,44). *HuR* is ubiquitously expressed, while the other human ELAV family proteins, HuB, HuC, and HuD, are limitedly expressed in the neuronal system or in the gonads (33,34). HuR directly binds to AREs and U-rich elements in the 3' UTR, intron sequences, or coding region of the pre-mRNA and mRNAs for regulation of pre-mRNA processing, stability, and translation of mRNA (45). HuR generally stabilizes mRNA by controlling both the processing of pre-mRNA and the stability of mature mRNA (45), which results in enhanced expression of the target proteins.

Consistently, HuR also competes with Ago2 and miRNA binding to the target mRNA, which promotes the translation of the mRNA when the HuR binding site is located close to Ago2-binding sites (46). However, the opposite regulatory function of HuR in cooperation with miRNA is also known. For example, *MYC*, *RhoB*, *SOX2*, and *p16* mRNAs are repressed by let-7, miR-19, and miR-145, respectively, in combination with the RNA-induced silencing complex (RISC) and HuR (47-50). It is unknown what mechanism determines the direction of HuR function, collaboration, or competition with miRNA and RISC, but the distance between the HuR-binding site and miRNA-binding site on mRNA or the conformation of mRNA is believed to shape the HuR function (43). This reported evidence supports our findings of HuR function in the repression of Top1 translation.

While we analyzed HuR binding to the eight ATTTA motifs existing in mouse *Top1* mRNA by RNA-IP, we were unable to identify the exact HuR binding sites in *Top1* mRNA by this method, as the many primer sets suggested the similar level of HuR recruitment to *Top1* mRNA. The ATTTA motif at the 3' end of 3'UTR seems to show reproducibly higher signal especially in the AID-

activated cells, which are CIT-stimulated CH12 cells and WT spleen B cells, showing some AID-dependent mechanism of HuR-binding to Top1 mRNA. However, more precise dissection of the HuR-binding sites in Top1 mRNA will be difficult, because the difference between the cells with and without AID is marginal and many AU-rich elements (WTTTW, W = A or T), other than ATTTA, are found in Top1 mRNA.

The function of Top1 is the maintenance of a DNA duplex by removing helical stress, so it is reasonable that Top1 is required for cell survival in multicellular organisms like *Drosophila melanogaster* and mice, while its orthologues, type I DNA topoisomerases, are dispensable in single-cell organisms such as bacteria and yeasts (51). Accordingly, *Top1* expression is supposed to be ubiquitous and stably expressed for cell maintenance. In contrast, many of the genes regulated by ARE binding factors through AREs in their 3' UTR represent inflammatory cytokines and growth factors that are responsive to stimulation and cellular stresses. Disturbed regulation of their expression may cause developmental abnormalities or diseases (52). Therefore, it is surprising that *Top1* gene translation, which is supposed to be rather stable, is actually finely tuned by HuR through AREs.

Observation using the UCSC genome browser shows that the 3' UTR of the *Top1* gene is conserved among vertebrates, as opposed to the 3' UTR of the *aicda* gene, for example (**Supplementary Figure 7**). *Aicda* gene expression is largely regulated at the transcriptional level by a combination of transcription factors such as NF- $\kappa$ B, c-Myb, and so on (53). Even in *Drosophila*, the 3' UTR of DNA of the *Top1* gene is reportedly 64% AU-rich and contains 8 copies of AUUUA motifs, compared to a 46% AU-rich coding region (51). In our HuR-immunoprecipitation results, HuR constitutively binds to the 3' end part of the 3' UTR of *Top1* mRNA, while AID activation doubles the frequency of *HuR* binding (**Fig. 4F, 4H**). Conservation of the sequence of the 3' UTR of the *Top1* gene and HuR binding in steady state to *Top1* mRNA suggests that ARE motifs in *Top1* mRNA may have another function relating to the response to some stimulation than AID-dependent DNA cleavage.

HuR was previously reported to be required for antigen-specific antibody production by regulating the oxidative stress response or germinal center maintenance using a *HuR* conditional knockout (cKO) mouse in combination with MB1-Cre or AID-Cre (31,41). In deletion of *HuR* gene by MB1-Cre, *HuR* was deleted after the pro-B cell stage, and cKO mice showed a decrease of production of antigen-specific IgG1 and IgG3, as well as the numbers of activated B cells and IgG1-positive cells. These disturbances in activated B cells are mainly caused by an abnormal splicing pattern of dihydrolipoamide S-succinyl transferase (*Dlst*) mRNA, resulting in decreased survival and proliferation capacity of the cKO primary B cells. Therefore, ROS scavengers rescue B cell proliferation and CSR defects in the *HuR* cKO primary B cells (31). AID-Cre-deleted *HuR* cKO cells showed no impairment in CSR ability, which probably occurred because the timing of the deletion of

*HuR* is after AID activation and it is too late to cause defective CSR efficiency. However, they showed decreased cell survival a few days after the deletion of *HuR* because of the altered splicing and abundance of many proteins, including c-Myc.

On the other hand, in *HuR*-KO CH12 cells, cell cycle disturbance is not observed and the ROS scavenger drugs do not rescue the impairment of CSR at all, whereas Dlst protein expression is decreased in *HuR*-KO cells. Additionally, c-Myc protein expression is not decreased. It is speculated that this CH12, the B lymphoma-derived cell line could overcome the ROS stress and cell cycle disturbances. This presumably occurs because CH12 cells have acquired the resistance against the general risks for cell survival during development into lymphoma. By using these cells, we identified another reason for CSR deficiency in *HuR*-deficient cells aside from cell cycle regulation and ROS stress.

Further analysis is needed to determine the precise molecular mechanism of HuR regulating AID-dependent translational suppression of *Top1*. Translational control by ARE-binding proteins is suggested to be associated with the poly(A) binding protein complex and translation initiation complex binding to the 5' UTR in general (52). It is also possible that HuR is associated with RISC, including Ago2 and some miRNAs. In the case of *Drosophila*, the two different poly(A) signals in *Top1* mRNA are used, and two types of *Top1* mRNA with different length are produced in different the developmental stages (51). Therefore, the change of HuR binding to some translation-related protein complexes or length alteration of *Top1* mRNA by AID activation will more precisely elucidate the molecular mechanism of the regulation of *Top1* protein synthesis by HuR.

## **Funding**

This work was supported by the Japan Society for Promotion of Science, KAKENHI, Grant Numbers JP22H00449 to TH and JP22K06202 to MK.

## **Acknowledgements**

We are grateful to Ms. Yoko Kitawaki, Dr. Misao Takemoto, and Ms. Maki Sasanuma for their invaluable technical support. We would also like to thank the past and present members of our laboratory for helpful discussions and comments about the manuscript and kindly sharing reagents.

## **Author contributions:**

M.K. designed the experiment. W.A., S.N., and M.K. performed the experiments and analyzed the data. W.A., M.K., S.N., and T.H. wrote the manuscript.

## **Conflicts of interest statement:**

All authors declare no conflicts of interest.

Accepted Manuscript

**Table**

**Table 1. Hypermutation analysis of 5'S $\mu$  region in *HuR*- and *HuR*+ cells**

	Mutation Frequency (/10 <sup>4</sup> bp)	Mutated bases / Total bases	Mutated clones / Total clones	Insert (clone) / deletion (clones)	IgA % (48h)
<b>CIT</b>	3.9 <sup>d</sup>	17 / 43,760	17/80	0 / 14 (11)	28.48
<b><i>HuR</i>- 4-OHT</b>	2.6 <sup>e</sup>	13 / 49,230	13/90	0 / 34 (12)	9.63
<b>no stim.</b>	2.1 <sup>f</sup>	9 / 43,760	9/80	0 / 7 (6)	0.25
<b>CIT</b>	8.9 <sup>a</sup>	46 / 51,418	30/94	1 (1) / 10 (8)	62.57
<b><i>HuR</i>+ 4-OHT</b>	7.9 <sup>b</sup>	29 / 36,649	24/67	0 / 7 (7)	31.34
<b>no stim.</b>	2.0 <sup>c</sup>	10 / 49,230	10/90	0 / 3 (3)	0.87

no stim., sample without stimulation.

a vs. d, P < 0.01; b vs. e, P < 0.001; c vs. f, P > 0.05;

a vs. c, P < 0.001; b vs. c, P < 0.001; d vs. f, P > 0.05; e vs. f, P > 0.05

## References

- 1 Honjo, T. and Kataoka, T. 1978. Organization of immunoglobulin heavy chain genes and allelic deletion model. *Proc Natl Acad Sci U S A* 75:2140.
- 2 Shimizu, A., Takahashi, N., Yaoita, Y., and Honjo, T. 1982. Organization of the constant-region gene family of the mouse immunoglobulin heavy chain. *Cell* 28:499.
- 3 Arakawa, H., Hauschild, J., and Buerstedde, J. M. 2002. Requirement of the activation-induced deaminase (AID) gene for immunoglobulin gene conversion. *Science* 295:1301.
- 4 Muramatsu, M., Kinoshita, K., Fagarasan, S., Yamada, S., Shinkai, Y., and Honjo, T. 2000. Class switch recombination and hypermutation require activation-induced cytidine deaminase (AID), a potential RNA editing enzyme. *Cell* 102:553.
- 5 Revy, P., Muto, T., Levy, Y., Geissmann, F., Plebani, A., Sanal, O., Catalan, N., Forveille, M., Dufourcq-Labeau, R., Gennery, A., Tezcan, I., Ersoy, F., Kayserili, H., Ugazio, A. G., Brousse, N., Muramatsu, M., Notarangelo, L. D., Kinoshita, K., Honjo, T., Fischer, A., and Durandy, A. 2000. Activation-induced cytidine deaminase (AID) deficiency causes the autosomal recessive form of the Hyper-IgM syndrome (HIGM2). *Cell* 102:565.
- 6 Begum, N. A., Nagaoka, H., Kobayashi, M., and Honjo, T. 2015. Chapter 18 - Molecular Mechanisms of AID Function. In Alt, F. W., Honjo, T., Radbruch, A., and Reth, M., eds., *Molecular Biology of B Cells (Second Edition)*, p. 305. Academic Press, London.
- 7 Begum, N. A., Kinoshita, K., Kakazu, N., Muramatsu, M., Nagaoka, H., Shinkura, R., Biniszkiwicz, D., Boyer, L. A., Jaenisch, R., and Honjo, T. 2004. Uracil DNA glycosylase activity is dispensable for immunoglobulin class switch. *Science* 305:1160.
- 8 Begum, N. A., Izumi, N., Nishikori, M., Nagaoka, H., Shinkura, R., and Honjo, T. 2007. Requirement of non-canonical activity of uracil DNA glycosylase for class switch recombination. *J Biol Chem* 282:731.
- 9 Begum, N. A., Stanlie, A., Doi, T., Sasaki, Y., Jin, H. W., Kim, Y. S., Nagaoka, H., and Honjo, T. 2009. Further evidence for involvement of a noncanonical function of uracil DNA glycosylase in class switch recombination. *Proc Natl Acad Sci U S A* 106:2752.
- 10 Yousif, A. S., Stanlie, A., Mondal, S., Honjo, T., and Begum, N. A. 2014. Differential regulation of S-region hypermutation and class-switch recombination by noncanonical functions of uracil DNA glycosylase. *Proc Natl Acad Sci U S A* 111:E1016.
- 11 Xu, J., Husain, A., Hu, W., Honjo, T., and Kobayashi, M. 2014. APE1 is dispensable for S-region cleavage but required for its repair in class switch recombination. *Proceedings of the National Academy of Sciences* 111:17242.
- 12 Islam, H., Kobayashi, M., and Honjo, T. 2019. Apurinic/aprimidinic endonuclease 1 (APE1) is dispensable for activation-induced cytidine deaminase (AID)-dependent somatic hypermutation in the immunoglobulin gene. *Int Immunol* 31:543.
- 13 Kobayashi, M., Aida, M., Nagaoka, H., Begum, N. A., Kitawaki, Y., Nakata, M., Stanlie, A., Doi, T., Kato, L., Okazaki, I. M., Shinkura, R., Muramatsu, M., Kinoshita, K., and Honjo, T. 2009. AID-induced decrease in topoisomerase I induces DNA structural alteration and DNA cleavage for class switch recombination. *Proc Natl Acad Sci U S A* 106:22375.
- 14 Kobayashi, M., Sabouri, Z., Sabouri, S., Kitawaki, Y., Pommier, Y., Abe, T., Kiyonari, H., and Honjo, T. 2011. Decrease in topoisomerase I is responsible for activation-induced cytidine deaminase (AID)-dependent somatic hypermutation. *Proc Natl Acad Sci U S A* 108:19305.

- 15 Vasudevan, S. and Peltz, S. W. 2001. Regulated ARE-mediated mRNA decay in *Saccharomyces cerevisiae*. *Mol Cell* 7:1191.
- 16 von Roretz, C. and Gallouzi, I. E. 2008. Decoding ARE-mediated decay: is microRNA part of the equation? *J Cell Biol* 181:189.
- 17 Barreau, C., Paillard, L., and Osborne, H. B. 2005. AU-rich elements and associated factors: are there unifying principles? *Nucleic Acids Res* 33:7138.
- 18 Nakamura, M., Kondo, S., Sugai, M., Nazarea, M., Imamura, S., and Honjo, T. 1996. High frequency class switching of an IgM<sup>+</sup> B lymphoma clone CH12F3 to IgA<sup>+</sup> cells. *Int Immunol* 8:193.
- 19 Schwarzer, A., Emmrich, S., Schmidt, F., Beck, D., Ng, M., Reimer, C., Adams, F. F., Grasedieck, S., Witte, D., Kabler, S., Wong, J. W. H., Shah, A., Huang, Y., Jammal, R., Maroz, A., Jongen-Lavrencic, M., Schambach, A., Kuchenbauer, F., Pimanda, J. E., Reinhardt, D., Heckl, D., and Klusmann, J. H. 2017. The non-coding RNA landscape of human hematopoiesis and leukemia. *Nat Commun* 8:218.
- 20 Labun, K., Montague, T. G., Krause, M., Torres Cleuren, Y. N., Tjeldnes, H., and Valen, E. 2019. CHOPCHOP v3: expanding the CRISPR web toolbox beyond genome editing. *Nucleic Acids Res* 47:W171.
- 21 Concordet, J. P. and Haeussler, M. 2018. CRISPOR: intuitive guide selection for CRISPR/Cas9 genome editing experiments and screens. *Nucleic Acids Res* 46:W242.
- 22 Doench, J. G., Fusi, N., Sullender, M., Hegde, M., Vaimberg, E. W., Donovan, K. F., Smith, I., Tothova, Z., Wilen, C., Orchard, R., Virgin, H. W., Listgarten, J., and Root, D. E. 2016. Optimized sgRNA design to maximize activity and minimize off-target effects of CRISPR-Cas9. *Nat Biotechnol* 34:184.
- 23 Sanson, K. R., Hanna, R. E., Hegde, M., Donovan, K. F., Strand, C., Sullender, M. E., Vaimberg, E. W., Goodale, A., Root, D. E., Piccioni, F., and Doench, J. G. 2018. Optimized libraries for CRISPR-Cas9 genetic screens with multiple modalities. *Nat Commun* 9:5416.
- 24 Perez-Pinera, P., Kocak, D. D., Vockley, C. M., Adler, A. F., Kabadi, A. M., Polstein, L. R., Thakore, P. I., Glass, K. A., Ousterout, D. G., Leong, K. W., Guilak, F., Crawford, G. E., Reddy, T. E., and Gersbach, C. A. 2013. RNA-guided gene activation by CRISPR-Cas9-based transcription factors. *Nat Methods* 10:973.
- 25 Al Ismail, A., Husain, A., Kobayashi, M., Honjo, T., and Begum, N. A. 2017. Depletion of recombination-specific cofactors by the C-terminal mutant of the activation-induced cytidine deaminase causes the dominant negative effect on class switch recombination. *Int Immunol* 29:525.
- 26 Cong, L., Ran, F. A., Cox, D., Lin, S., Barretto, R., Habib, N., Hsu, P. D., Wu, X., Jiang, W., Marraffini, L. A., and Zhang, F. 2013. Multiplex genome engineering using CRISPR/Cas systems. *Science* 339:819.
- 27 Doi, T., Kato, L., Ito, S., Shinkura, R., Wei, M., Nagaoka, H., Wang, J., and Honjo, T. 2009. The C-terminal region of activation-induced cytidine deaminase is responsible for a recombination function other than DNA cleavage in class switch recombination. *Proc Natl Acad Sci U S A* 106:2758.
- 28 Lopez de Silanes, I., Zhan, M., Lal, A., Yang, X., and Gorospe, M. 2004. Identification of a target RNA motif for RNA-binding protein HuR. *Proc Natl Acad Sci U S A* 101:2987.
- 29 Tenenbaum, S. A., Lager, P. J., Carson, C. C., and Keene, J. D. 2002. Ribonomics: identifying mRNA subsets in mRNP complexes using antibodies to RNA-binding proteins and genomic arrays. *Methods* 26:191.
- 30 Gandin, V., Sikstrom, K., Alain, T., Morita, M., McLaughlan, S., Larsson, O., and Topisirovic, I. 2014. Polysome fractionation and analysis of mammalian translato-



- on a genome-wide scale. *J Vis Exp*.
- 31 Diaz-Munoz, M. D., Bell, S. E., Fairfax, K., Monzon-Casanova, E., Cunningham, A. F., Gonzalez-Porta, M., Andrews, S. R., Bunik, V. I., Zarnack, K., Curk, T., Heggermont, W. A., Heymans, S., Gibson, G. E., Kontoyiannis, D. L., Ule, J., and Turner, M. 2015. The RNA-binding protein HuR is essential for the B cell antibody response. *Nat Immunol* 16:415.
- 32 Gilbert, L. A., Horlbeck, M. A., Adamson, B., Villalta, J. E., Chen, Y., Whitehead, E. H., Guimaraes, C., Panning, B., Ploegh, H. L., Bassik, M. C., Qi, L. S., Kampmann, M., and Weissman, J. S. 2014. Genome-Scale CRISPR-Mediated Control of Gene Repression and Activation. *Cell* 159:647.
- 33 Cherry, J., Karschner, V., Jones, H., and Pekala, P. H. 2006. HuR, an RNA-binding protein, involved in the control of cellular differentiation. *In Vivo* 20:17.
- 34 Hinman, M. N. and Lou, H. 2008. Diverse molecular functions of Hu proteins. *Cell Mol Life Sci* 65:3168.
- 35 Stanlie, A., Begum, N. A., Akiyama, H., and Honjo, T. 2012. The DSIF subunits Spt4 and Spt5 have distinct roles at various phases of immunoglobulin class switch recombination. *PLoS Genet* 8:e1002675.
- 36 Shockett, P. and Stavnezer, J. 1991. Effect of cytokines on switching to IgA and alpha germline transcripts in the B lymphoma I.29 mu. Transforming growth factor-beta activates transcription of the unrearranged C alpha gene. *J Immunol* 147:4374.
- 37 Wu, X. P., Feng, J. L., Komori, A., Kim, E. C., Zan, H., and Casali, P. 2003. Immunoglobulin somatic hypermutation: Double-strand DNA breaks, AID and error-prone DNA repair. *J Clin Immunol* 23:235.
- 38 Schenten, D., Kracker, S., Esposito, G., Franco, S., Klein, U., Murphy, M., Alt, F. W., and Rajewsky, K. 2009. Pol zeta ablation in B cells impairs the germinal center reaction, class switch recombination, DNA break repair, and genome stability. *Journal of Experimental Medicine* 206:477.
- 39 Daly, J., Bebenek, K., Watt, D. L., Richter, K., Jiang, C. C., Zhao, M. L., Ray, M., McGregor, W. G., Kunkel, T. A., and Diaz, M. 2012. Altered Ig Hypermutation Pattern and Frequency in Complementary Mouse Models of DNA Polymerase zeta Activity. *Journal of Immunology* 188:5528.
- 40 Faili, A., Aoufouchi, S., Flatter, E., Gueranger, Q., Reynaud, C. A., and Weill, J. C. 2002. Induction of somatic hypermutation in immunoglobulin genes is dependent on DNA polymerase iota. *Nature* 419:944.
- 41 Osma-Garcia, I. C., Capitan-Sobrinho, D., Mouysset, M., Bell, S. E., Lebeurrier, M., Turner, M., and Diaz-Munoz, M. D. 2021. The RNA-binding protein HuR is required for maintenance of the germinal centre response. *Nat Commun* 12:6556.
- 42 Wang, W. G., Caldwell, M. C., Lin, S. K., Furneaux, H., and Gorospe, M. 2000. HuR regulates cyclin A and cyclin B1 mRNA stability during cell proliferation. *Embo Journal* 19:2340.
- 43 Srikantan, S., Tominaga, K., and Gorospe, M. 2012. Functional interplay between RNA-binding protein HuR and microRNAs. *Curr Protein Pept Sci* 13:372.
- 44 Ma, W. J., Cheng, S., Campbell, C., Wright, A., and Furneaux, H. 1996. Cloning and characterization of HuR, a ubiquitously expressed Elav-like protein. *J Biol Chem* 271:8144.
- 45 Mukherjee, N., Corcoran, D. L., Nusbaum, J. D., Reid, D. W., Georgiev, S., Hafner, M., Ascano, M., Jr., Tuschl, T., Ohler, U., and Keene, J. D. 2011. Integrative regulatory mapping indicates that the RNA-binding protein HuR couples pre-mRNA processing and mRNA stability. *Mol Cell* 43:327.
- 46 Lu, Y. C., Chang, S. H., Hafner, M., Li, X., Tuschl, T., Elemento, O., and Hla, T. 2014.

- ELAVL1 modulates transcriptome-wide miRNA binding in murine macrophages. *Cell Rep* 9:2330.
- 47 Chang, N., Yi, J., Guo, G., Liu, X., Shang, Y., Tong, T., Cui, Q., Zhan, M., Gorospe, M., and Wang, W. 2010. HuR uses AUF1 as a cofactor to promote p16INK4 mRNA decay. *Mol Cell Biol* 30:3875.
- 48 Glorian, V., Maillot, G., Poles, S., Iacovoni, J. S., Favre, G., and Vagner, S. 2011. HuR-dependent loading of miRNA RISC to the mRNA encoding the Ras-related small GTPase RhoB controls its translation during UV-induced apoptosis. *Cell Death Differ* 18:1692.
- 49 Kim, H. H., Kuwano, Y., Srikantan, S., Lee, E. K., Martindale, J. L., and Gorospe, M. 2009. HuR recruits let-7/RISC to repress c-Myc expression. *Genes Dev* 23:1743.
- 50 Latorre, E., Carelli, S., Caremoli, F., Giallongo, T., Colli, M., Canazza, A., Provenzani, A., Di Giulio, A. M., and Gorio, A. 2016. Human Antigen R Binding and Regulation of SOX2 mRNA in Human Mesenchymal Stem Cells. *Mol Pharmacol* 89:243.
- 51 Brown, S. D., Zhang, C. X., Chen, A. D., and Hsieh, T. S. 1998. Structure of the Drosophila DNA topoisomerase I gene and expression of messages with different lengths in the 3' untranslated region. *Gene* 211:195.
- 52 Otsuka, H., Fukao, A., Funakami, Y., Duncan, K. E., and Fujiwara, T. 2019. Emerging Evidence of Translational Control by AU-Rich Element-Binding Proteins. *Front Genet* 10:332.
- 53 Tran, T. H., Nakata, M., Suzuki, K., Begum, N. A., Shinkura, R., Fagarasan, S., Honjo, T., and Nagaoka, H. 2010. B cell-specific and stimulation-responsive enhancers derepress Aicda by overcoming the effects of silencers. *Nat Immunol* 11:148.

Accepted Manuscript

## Figure Legends

### **Fig. 1. The screening of the major AU-rich element binding proteins identified *HuR/ELAVL1* as the factor required in CSR.**

(A) The knockdown effect of the major ARE binding factors, *Brf1*, *Brf2*, *hnRNPD*, *Khsrp*, *Zfp36*, and *HuR* on CSR to IgA. CRISPR interference was used for knockdown except for *HuR*. CSR to IgA at 24 hours after the start of CIT stimulation was evaluated. The mean  $\pm$  SD values calculated from three independent experiments are shown. CIT, cytokine cocktail of CD40L, IL-4, and TGF $\beta$ . NS, no-stimulation samples.

(B) Expression level of each molecule after knockdown shown in (A). The q-PCR signal was normalized by  $\beta$ 2M while *Gapdh* was used for *HuR* and the control sample (=1).

(C) *AID* mRNA expression in the cells shown in (A) measured by qPCR.

(D)  $\mu$ - and  $\alpha$ -germline transcripts (*GLT*) of the switch regions in the cells shown in (A).

### **Fig. 2. *HuR* positively contributes to *IgH* gene diversification by regulating the DNA cleavage frequency.**

(A) *HuR* expression detected by western blot in *HuR* knockout (KO) cell lines #101 and #111 stably transfected by the 3XFLAG-tagged *HuR* (*HuR*<sup>+</sup>) or empty vectors (*HuR*<sup>-</sup>) with or without stimulation by CIT. *AID* expression is also shown.  $\alpha$ tubulin is a loading control. Wild-type cell lysate is from the wild-type CH12 cells. no stim., without stimulation.

(B) IgA% (the mean  $\pm$  SD) at 24 (top) and 48 (bottom) hours from the start of CIT stimulation in the #101 and #111 cell lines with or without replacement of *HuR*. P-values in CSR evaluation were calculated by student *t*-test. \*, P < 0.05; \*\*, P < 0.01.

(C) Representative flowcytometric patterns of IgA (left) or IgG3 (right) expression of the selected clones #22B (*HuR*<sup>-</sup>) and #11A (*HuR*<sup>+</sup>). IgA% and IgG3% were detected at 72 hours from the start of stimulation. no stim., without stimulation. CI, stimulation with CD40L and IL-4. SSC, side scattered.

(D-E) The mean  $\pm$  SD of IgA% (D) and IgG3% (E) of *HuR*<sup>-</sup> (22B) and *HuR*<sup>+</sup> (11A) cells at the indicated time points of the five to six independent experiments. \*\*\*, P < 0.001.

(F) The analyzed region mutated by AID-dependent hypermutation (G).

(G) Mutation frequency of *HuR*<sup>-</sup> and *HuR*<sup>+</sup> cells. P values were calculated by Fisher's exact test. \*\*, P < 0.01; \*\*\*, P < 0.001; n.s., not significant.

(H) DNA break assay using biotinylated d-UTP (Bio-dUTP) labeling by terminal deoxynucleotidyl transferase. *HuR*<sup>+</sup> and *HuR*<sup>-</sup> cells with or without CIT stimulation were used. CIT-stimulated AID-knockout cells and *HuR*<sup>+</sup> cells without labeling were used as negative control. The primers are described in **Supplementary Table 1**.

**Fig. 3. Reduced efficiencies of CSR, SHM, and DNA cleavage in *HuR*-deficient cells are not due to the defect of cell cycle progression or oxidative stress responses.**

(A-C) Cell cycle analysis with CellTrace Violet dye (CTV) using the monoclonal #22B *HuR*<sup>-</sup> and #11A *HuR*<sup>+</sup> CH12 cells.

(A) Time course of the cell proliferation assay and CIT stimulation. The cells were incubated with CTV in their culture medium following CIT stimulation while aphidicolin samples were unstimulated.

(B) IgA% in the cells used in the CTV cell proliferation assay. The mean ± SD is shown.

(C) Representative histogram of *HuR*<sup>-</sup> (blue) and *HuR*<sup>+</sup> (red) cells labelled by CTV. Whole cells (left) or switched (IgA<sup>+</sup>) (right) populations are shown. *HuR*<sup>-</sup> without stimulation was incubated with aphidicolin to monitor the cell division. Inset shows the result of *HuR*<sup>-</sup>, non-stimulated cells incubated with (green) or without (magenta) aphidicolin. no stim., not stimulated.

(D-F) The effects of reactive oxygen species (ROS) scavenger drugs on CSR in *HuR*<sup>-</sup> and *HuR*<sup>+</sup> cells derived from #111 *HuR*-KO clones.

(D) Time course for IgA% and dead cell% analyses with two ROS scavenger drugs, N-Acetyl-L-Cysteine (L-NAC) and chloro[[2,2'-[1,2-ethanediy]bis[(nitri]lo-κN)methylidyne]]bis[6-methoxyphenolato-κO]]-manganese (EUK-134).

(E-F) Analysis of CSR to IgA (**top**) and dead cells (**bottom**) exposed to the serial concentration of L-NAC (E, 0 - 50 mM) or EUK-134 (F, 0 - 10 mM) in *HuR*<sup>-</sup> and *HuR*<sup>+</sup> cells. Gray triangles show the increment of the concentration of the drugs.

(G) Detection of the inclusion of *Intron (Int) 10* of dihydroipoamide S-succinyltransferase (*Dlst*) mRNA evaluated by qPCR with the two primer sets covering exon-intron boundaries in #22B, *HuR*<sup>-</sup> and #11A, *HuR*<sup>+</sup> cells. The signals from the specific primers were normalized by the signals of *Gapdh* mRNA. The mean ± SD of each primer set of three independent experiments. The arrows show the primers amplifying *Exon (Ex) 10- Int 10* transcripts, and the triangles show the primers

amplifying *Int 10-Ex 11* transcripts. \*, P < 0.05; \*\*, P < 0.01; n.s., not significant; no stim., without stimulation.

**(H)** Conventional RT-PCR analysis amplifying *Ex 10-Ex 11* evaluating alternative splicing in *Dlst* mRNA. *Exon 10b (Ex 10b)* is an unusual cryptic exon described by Diaz-Muñoz et al. (31).

**(I-J)** Representative western blot images of *Dlst* **(I)** and c-Myc **(J)** protein expression in stimulated or non-stimulated *HuR*<sup>-</sup> and *HuR*<sup>+</sup> cells out of three experiments. GAPDH **(I)** and β-actin **(J)** are loading controls.

**Fig. 4. AID-dependent repression of *Top1* is eliminated in *HuR*-deficient cells.**

**(A-B)** *Top1* protein change by CIT or CI stimulation in #22B *HuR*<sup>-</sup> and #11A *HuR*<sup>+</sup> cells. The proteins were extracted by PBS with TritonX-100 **(A)** or RIPA **(B)** buffer. GAPDH is the loading control.

**(C)** *Top1* mRNA expression in #22B *HuR*<sup>-</sup> and #11A *HuR*<sup>+</sup> cells with or without CIT or CI stimulation analyzed by q-PCR. The mean ± SD of *Top1* mRNA signals normalized by *Gapdh* mRNA is shown.

**(D)** Mouse *Top1* mRNA structure and the position of the eight ATTTA motifs. The primer set position (*a* ~ *h*) used for q-PCR in RNA-IP experiments **(E-H)** are shown by the bars.

**(E-F)** RNA-IP analysis using #11A *HuR*<sup>+</sup> cells and anti-HuR antibody.

**(E)** Western blot analysis showing the immunoprecipitation (IP) efficiency.

**(F)** Enrichment of *Top1*, *Gapdh*, or *c-Myc* mRNA to HuR protein evaluated by q-PCR. The mean ± SD values of the three independent experiments are shown.

**(G-H)** RNA-IP analysis using wildtype and AID knockout mice spleen B cells and anti-HuR antibody after stimulation with LPS and IL-4 for four days.

**(G)** Western blot analysis showing the immunoprecipitation (IP) efficiency.

**(H)** Enrichment of *Top1*, *Gapdh*, or *c-Myc* mRNA by HuR protein evaluated by q-PCR. The mean ± SD values of the two independent experiments are shown.

**(I-N)** Polysome analysis comparing CIT-stimulated and unstimulated #22B *HuR*<sup>-</sup> and #11A *HuR*<sup>+</sup> cells.

(I-J) Optical density (OD) was measured at 256 nm in the fractions (#1-#90) obtained by ultracentrifuging of the 10-45% sucrose gradient in CIT-stimulated or unstimulated *HuR*<sup>-</sup> (I) or *HuR*<sup>+</sup> cells (J).

(K-N) RNA analysis of the pooled samples collected from 10 serial fractions. *Top1* mRNA in *HuR*<sup>-</sup> (K) or *HuR*<sup>+</sup> cells (L). *b2M* mRNA in *HuR*<sup>-</sup> (M) or *HuR*<sup>+</sup> cells (N). Grey triangles show the change of the sucrose concentration of the pooled samples.

**Fig. 5. Knockdown of *Top1* rescues the impairment of CSR to IgG3 completely and CSR to IgA partially in *HuR*-deficient cells.**

(A) Time course of *Top1* knockdown experiments.

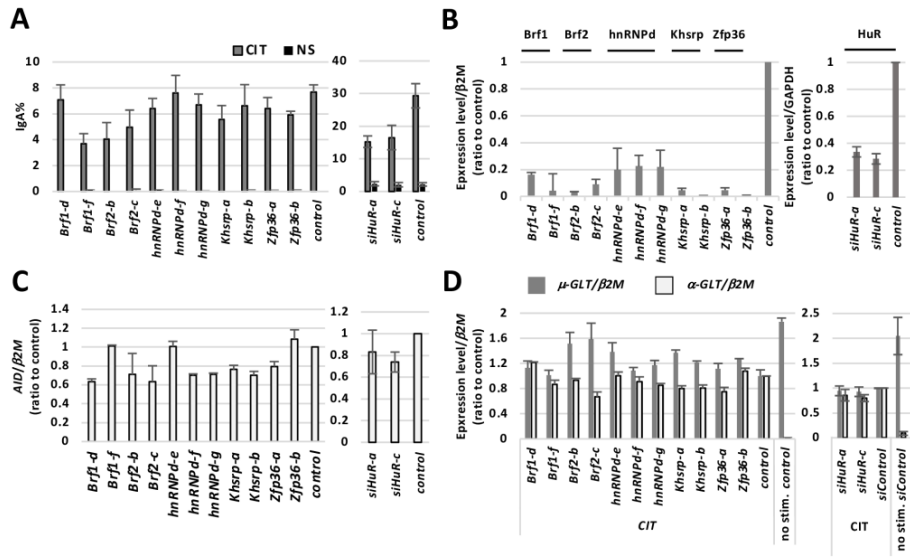
(B) Western blot analysis for Top1 protein expression after repeated si*Top1*. Actin was used as a loading control.  $1.6$  or  $3.2 \times 10^5$  cells/lane were loaded in si*Top1*, and  $0.8$  or  $1.6 \times 10^5$  cells/lane were loaded in siControl.

(C) Representative flowcytometric pattern of CSR to IgA (left two rows) and IgG3 (right two rows). *HuR*<sup>-</sup> or *HuR*<sup>+</sup> cells stimulated with CI or CIT for 72 hours transfected with or without 3 mM si*Top1*.

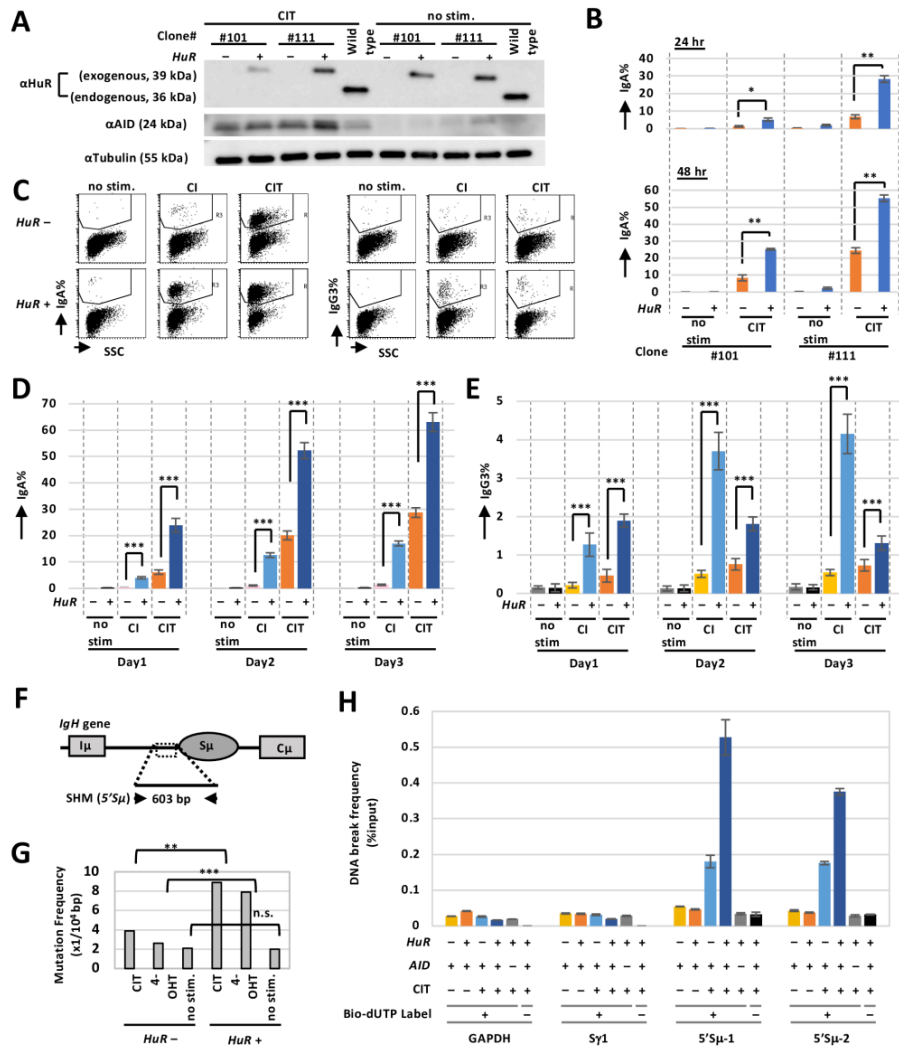
(D-E) The mean  $\pm$  SD of IgA% (D) and IgG3% (E) from six and three independent experiments, respectively, observed from days 1 to 3. \*,  $P < 0.05$ ; \*\*,  $P < 0.01$ ; \*\*\*,  $P < 0.001$ ; n.s., not significant.

**Fig. 6. *HuR* is required for decrease in *Top1*, DNA cleavage, and CSR.** When amount of Top1 protein is decreased by the repeated knockdown of *Top1*, *HuR*-deficient cells show “rescue” of CSR efficiency to the level of *HuR*-proficient cells in CSR to IgG3. The reason for this rescue may be that the equally minimized amount of Top1 protein in both *HuR*-deficient and -proficient cells achieved similarly sufficient levels of altered non-B DNA structure and DNA cleavage.

**Fig.1**

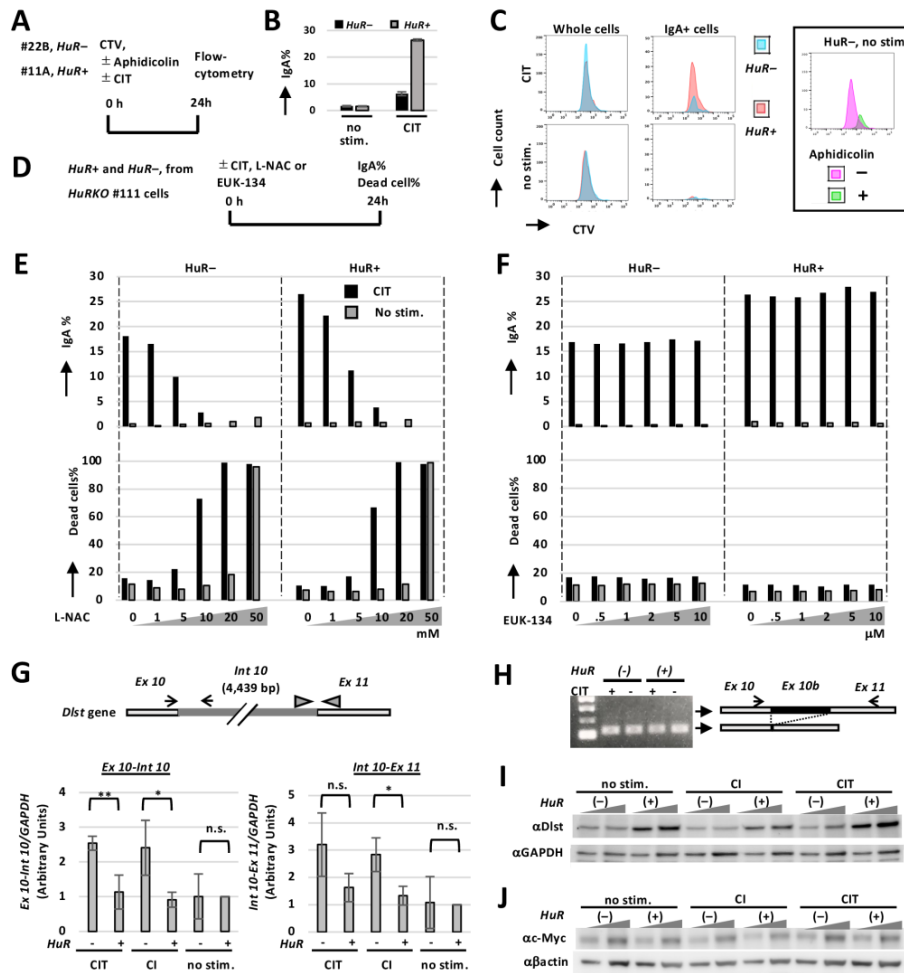


**Fig. 2**

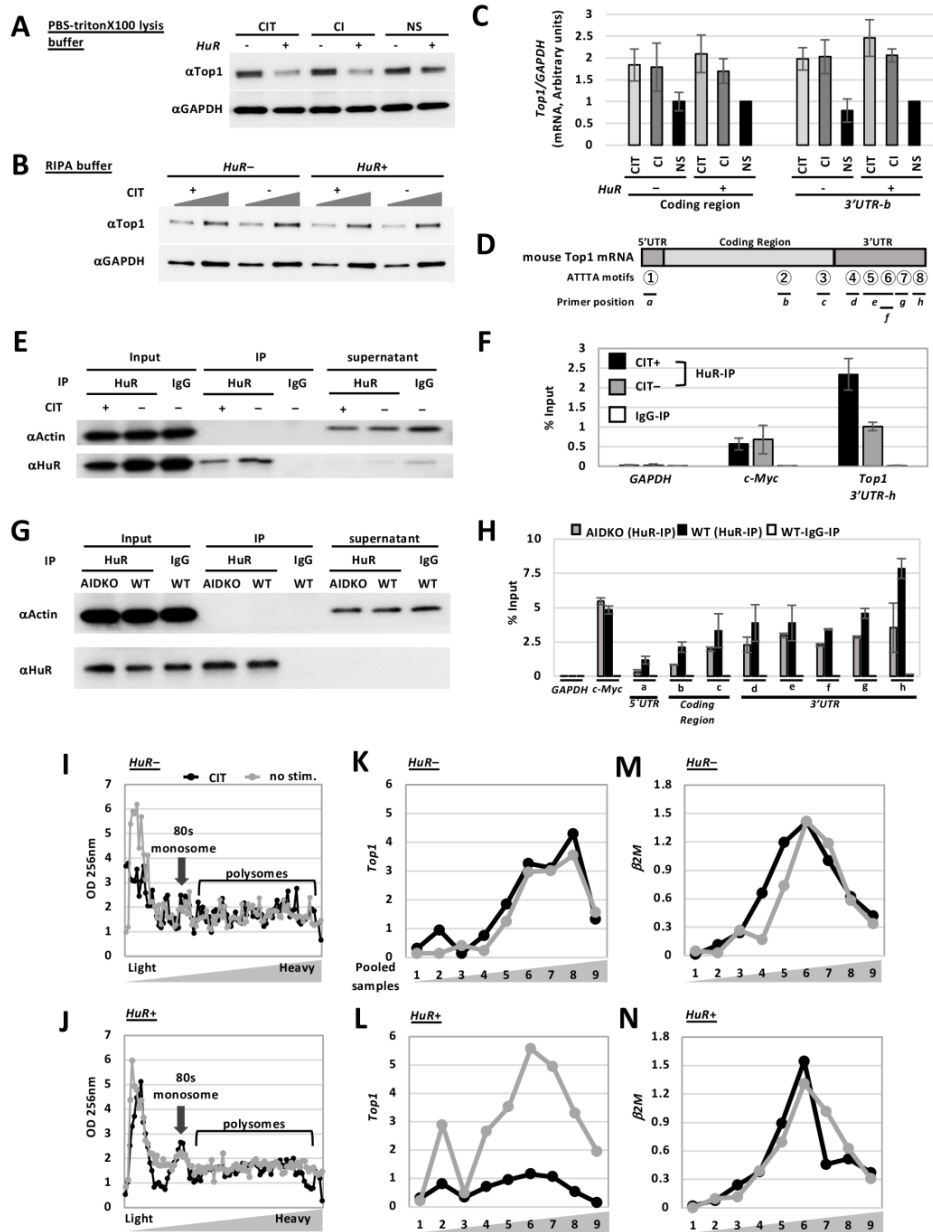




**Fig. 3**









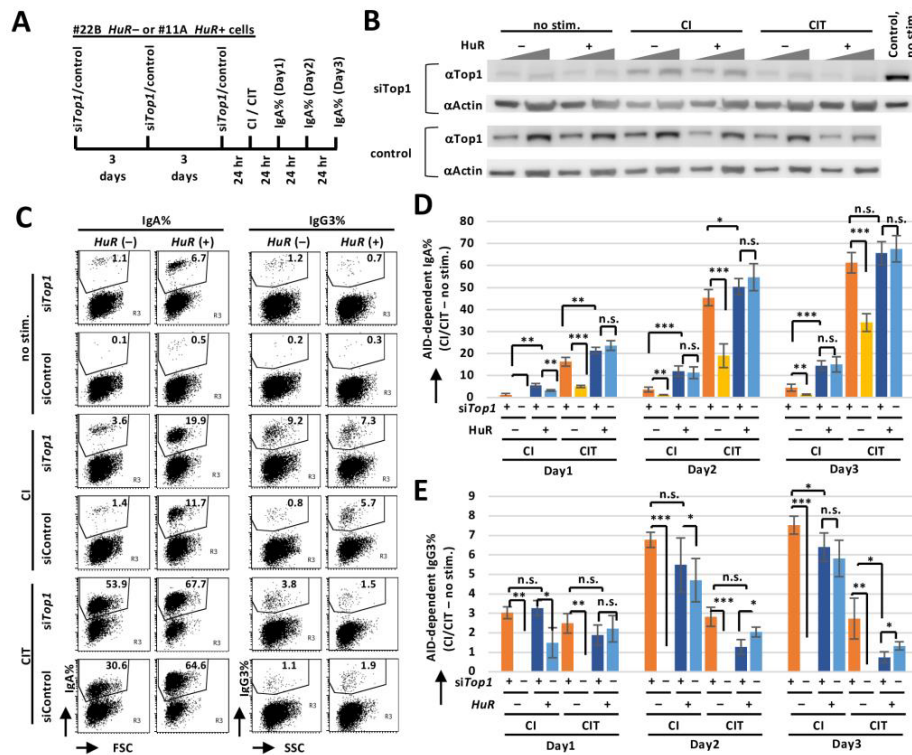


**Fig.4**



**Fig.5**



**Fig.6**

	<b>HuR-proficient</b>		<b>HuR-deficient</b>	
	<b>No siTop1</b>	<b>Repeated siTop1</b>	<b>No siTop1</b>	<b>Repeated siTop1</b>
<b>Soluble Top1 protein</b>				
<b>AID-dependent Top1 decrease</b>	effective	No further effect	no	no
<b>Soluble Top1 after AID activation</b>				
<b>NonB DNA (supposed)</b>	sufficient	sufficient	low	sufficient
<b>CSR to IgG3</b>	normal	Increased ~ normal	none	Rescued to HuR-proficient level!
<b>CSR to IgA</b>	normal	Increased ~ normal	low	low ~ nearly normal